CWhatUC : A Visual Acuity Simulator

Daniel D. Garcia[a], Brian A. Barsky[a,b], Stanley A. Klein[b]

[a]University of California, EECS Computer Science Division, 387 Soda Hall # 1776,
Berkeley CA 94720-1776
[b]University of California, School of Optometry, 360 Minor Hall # 2020, Berkeley CA 94720-2020

ABSTRACT

CWhatUC (pronounced "see what you see") is a computer software system which will predict a patient's visual acuity using several techniques based on fundamentals of geometric optics. The scientific visualizations we propose can be clustered into two classes: retinal representations and corneal representations; however, in this paper, we focus our discussion on corneal representations. It is important to note that, for each method listed below, we can illustrate the visual acuity with or without spectacle correction. Corneal representations are meant to reveal how well the cornea focuses parallel light onto the fovea of the eye by providing a pseudo-colored display of various error metrics. These error metrics could be:

a) standard curvature representations, such as *instantaneous* or *axial curvature*, converted to refractive power maps by taking Snell's law into account
b) the *focusing distance* from each refracted ray's average focus to the computed fovea
c) the *retinal distance* on the retinal plane from each refracted ray to the chief ray (lateral spherical aberration)

For each error metric, we show both real and simulated data, and illustrate how each representation contributes to the simulation of visual acuity.

Keywords: visual acuity, ray tracing, corneal topography, scientific visualization, keratoconus, videokeratography

1. BACKGROUND

The cornea is the transparent tissue covering the front of the eye. It performs 3/4 of the refraction, or bending, of light in the eye, and focuses light towards the lens and the retina. Thus, subtle variations in the shape of the cornea can significantly diminish visual performance. Recently, instruments to measure corneal topography have become commercially available; they are known as videokeratographs (VKs).[1,2,3,4,5] These corneal topography devices typically shine rings of light onto the cornea and then capture the reflection pattern with a built-in video camera. Figure 1 shows the ring pattern from a patient whose visual acuity we wish to simulate.
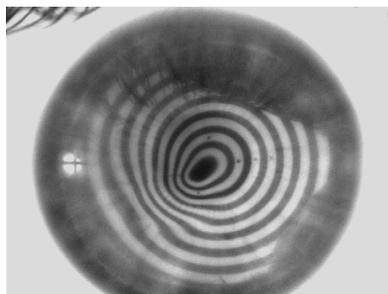

Figure 1: The reflection pattern from a patient with an irregularly-shaped cornea.

——————————————————
Further author information —
D.D.G.(correspondence): Email: ddgarcia@cs.berkeley.edu; WWW: http://www.cs.berkeley.edu/~ddgarcia/; Telephone: 510-642-9716; Fax: 510-642-5775
B.A.B.: Email: barsky@cs.berkeley.edu; WWW: http://www.cs.berkeley.edu/~barsky/; Telephone: 510-642-9838; Fax: 510-642-5775
S.A.K.: Email: klein@adage.berkeley.edu; WWW: http://spectacle.berkeley.edu/VSP/SK.html; Telephone: 510-643-8670; Fax: 510-643-5109
More information about this research can be found at http://www.cs.berkeley.edu/optical/ and the color images from the poster that accompanied this paper are at http://www.cs.berkeley.edu/optical/SPIE/

Instead of allowing the instrument to process the pattern, we extract the data and construct a mathematical spline surface representation from these reflection patterns[6,7]. This representation allows us to query, or "sample" the surface at arbitrary points to determine information about surface position, normals and principal curvatures. CWhatUC is a software system that uses this information to compute and display different metrics of visual acuity. A wireframe rendering of an example surface with a very low sampling density is shown in Figure 2.
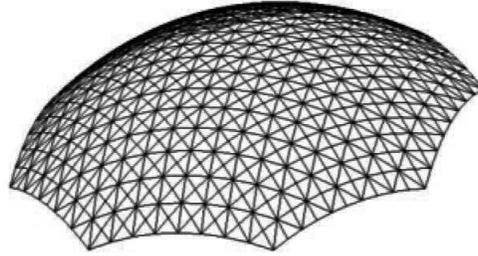

Figure 2: A wireframe rendering of a reconstructed mathematical spline surface.

2. THE FOUR METRICS

We propose four metrics to simulate the corneal contribution to visual acuity. Figure 3 illustrates how we compute the values that we use in our calculations. Our corneal model is a very simple one since we ignore the contribution of the lens and consider the entire cornea to be a uniform material with a constant index of refraction (n) of 1.3375. It is important to note that the metrics we propose here are independent of our implementation. If we were to improve the quality of the model, the metrics themselves would remain unchanged.
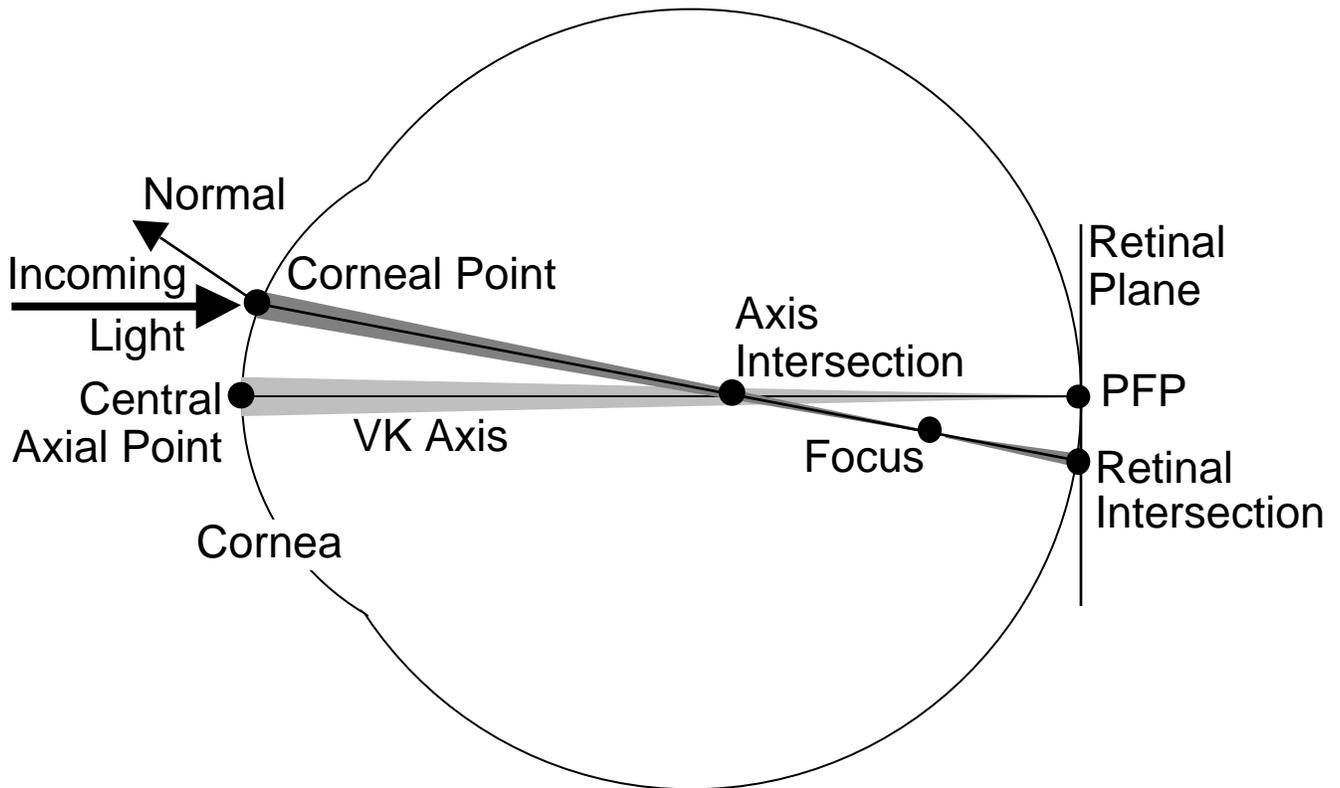

Figure 3: A simple model of the cornea, eye, and the refraction of a ray of incoming light.

We begin the computation at the central axial point on the cornea. We refract incoming parallel light and calculate where it converges to a focus using Coddington's equations[8,9]. Fortunately, due to constraints in our representation, the normal at the central point is parallel to the incoming parallel light; thus, according to Snell's law, the refracted light will also be in this same direction. If the central axial point has some astigmatism, or cylinder, then so will the refracted wavefront and there will be two principal curvatures. We define the paraxial focal point (PFP) to be the focus as determined by the average of these curvatures (also known as "mean sphere"). The VK axis, which is the z-axis, is the line from the central axial point to the PFP. The retinal plane is the plane that passes through the PFP and is normal to the VK axis.

Then, for each corneal point of interest, we refract parallel incoming light according to Snell's law and Coddington's equations and we calculate where that light focuses. Again, if there is any cylinder in the refracted wavefront, then there will be two principal curvatures; in that case, we use their average to determine the focus. The retinal intersection is the location where the refracted ray intersects the retinal plane. If the normal lies in the meridional plane[*], then the axis intersection is the intersection of the refracted ray with the VK axis; otherwise, the refracted ray will not intersect the VK axis. In that case, we choose the axis intersection to be the point of closest approach to the central axis along the refracted ray. At the central axial point there are infinitely many such intersections; thus, for that corneal point, we set the axis intersection to be the PFP.

2.1 Axial Refractive Power

We define axial refractive power at a corneal point to be the quotient of index of refraction of our model cornea divided by the distance from the corneal point to the axis intersection. This map often has a characteristic "figure-8" or "crescent" shape. Clinicians are familiar with this representation because it is similar to the standard axial curvature maps used in most corneal topography instruments. The acute asymmetry of the maps often facilitates the identification and measurement of the amount and orientation of astigmatism.

$$\text{Axial refractive power} \; = \frac{n}{\texttt{Distance3D(Corneal\_Point, Axis\_Intersection)}} \tag{1}$$

where

$$\texttt{Distance3D}(P_0, P_1) = \sqrt{\left(P_{1x} - P_{0x}\right)^2 + \left(P_{1y} - P_{0y}\right)^2 + \left(P_{1z} - P_{0z}\right)^2} \tag{2}$$
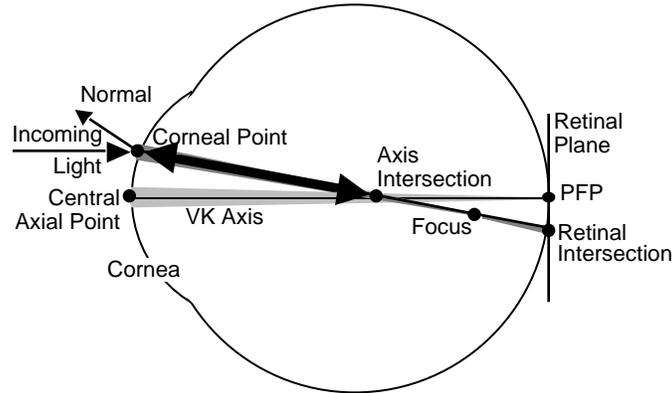

Figure 4: Axial refractive power is a function of the distance between the corneal point and the axis intersection.

This definition differs from the traditional axial curvature map[10,11,12] in that this refractive power map takes into account the refraction of an incoming parallel ray, whereas the standard map is purely a surface shape quantity. For example, the standard axial curvature of a sphere is constant over its surface, whereas the axial refractive power increases as we move away from the center. Figure 5 illustrates a direct comparison of these two quantities on a simulated cornea having with-the-rule astigmatism. Note that even though there is a difference in the orientation of the figure-8 pattern, they are identical in the central region near the VK axis.

---

[*] We define the meridional plane to be the plane containing the VK Axis and the corneal point.
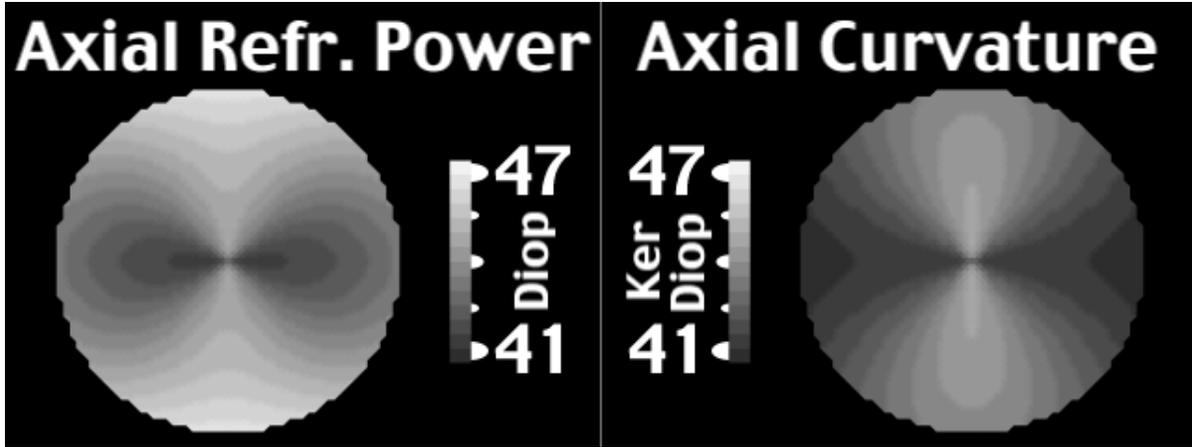
Figure 5: A comparison between axial refractive power and axial curvature.

2.2 Instantaneous Refractive Power

We define instantaneous refractive power at a corneal point to be the quotient of index of refraction of our model cornea divided by the focal distance of the cornea at that point, which is the distance from the corneal point to the focus. This is the only one of our four metrics that is not a function of the central axis or of the PFP; rather, it is purely a measure of the surface's refracting power. The advantage of this definition over other traditional representations such as mean sphere[13], Gaussian power[14,15], axial power, and instantaneous power is that this metric illustrates spherical aberration. Those other metrics would be constant for a sphere, whereas instantaneous refractive power increases away from the center.

$$\text{Instantaneous refractive power} \; = \; \frac{n}{\texttt{Distance3D(Corneal\_Point, Focus)}} \tag{3}$$
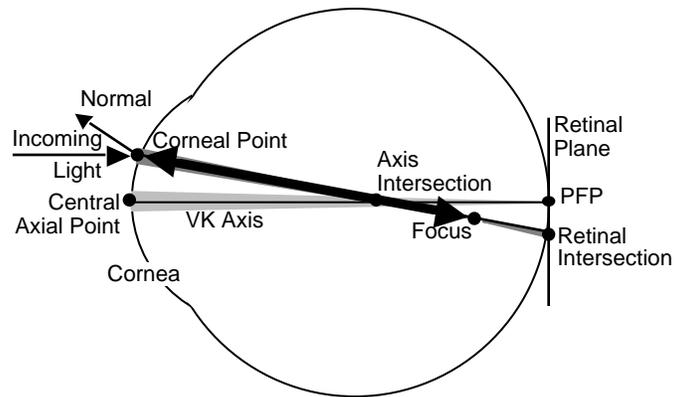

Figure 6: Instantaneous refractive power is a function of the distance between the corneal point and the focus.

2.3 Retinal Distance

We define the retinal distance, for each corneal point, to be the distance from the PFP to the retinal intersection, that is, to the point of intersection of the refracted ray with the retinal plane. Since the retinal plane was defined to contain the PFP, both the retinal intersection and the PFP lie in that plane; thus, the distance calculation is a two-dimensional planar distance measure. For a perfect eye, parallel light would converge to a point focus at the PFP and thus, in this case, the retinal distance at every corneal point would be zero. This metric provides an estimate of lateral spherical aberration.

$$\text{Retinal distance} = \texttt{Distance2D(Retinal\_Intersection, PFP)} \tag{4}$$

where

$$\mathtt{Distance2D}(P_0, P_1) = \sqrt{\left(P_{1x} - P_{0x}\right)^2 + \left(P_{1y} - P_{0y}\right)^2}$$ (5)
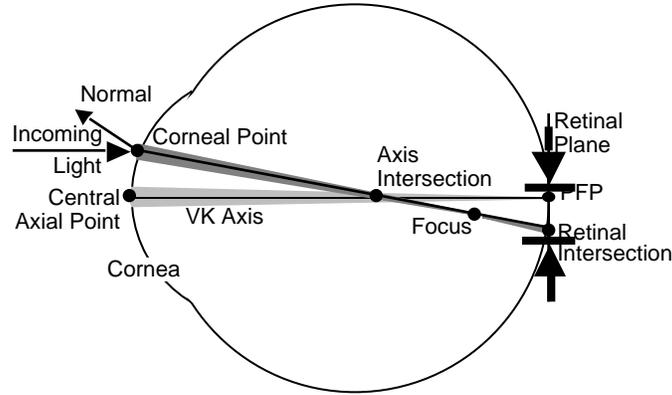

Figure 7: Retinal distance is the distance between the retinal intersection and the PFP.

2.4 Focusing Distance

We define focusing distance, for each corneal point, to be the distance from the focal point of the refracted ray to the PFP. For a perfect eye, the rays of incoming parallel light would converge to a point focus at the PFP and thus the focusing distance for every corneal point would be zero in this case.

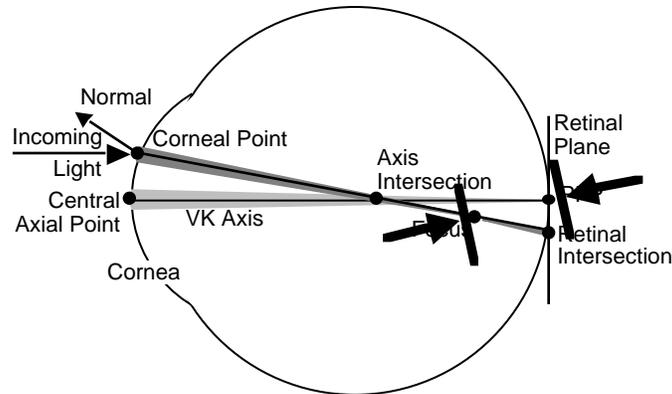$$\text{Focusing distance} = \mathtt{Distance3D(Focus,\ PFP)}$$ (6)

Figure 8: Focusing distance is the distance between the focus and the PFP.

3. REPRESENTATIONS

For each acuity metric, we determine the minimum and maximum values over all the points on the cornea, define a colormap to span those values, and index into that colormap to pseudo-color the surface of the cornea. We have chosen a grey-scale map here, but a user of CWhatUC is provided with a full-color map.[**]

[**] Note that the hardcopy halftoning has introduced some visible non-linearity to the grey-scale map. This is not an artifact of the data, but of the printing process itself. This is most easily seen in Figure 10 of the simulated data; the actual instantaneous refractive power and focusing distance maps are smooth and do not have a "ring" halfway out as the images would suggest.

4. RESULTS

We display our four metrics on two sets of data, a simulated cornea and a real cornea. The four metrics each contribute some information to the clinician about the projected visual acuity, as we will see.

4.1 Simulated Data

We use a simple asymmetric ellipsoid to simulate a cornea that has with-the-rule astigmatism. The equation for the ellipsoid is

$$\frac{x}{A}^2 + \frac{y}{B}^2 + \frac{C-z}{C}^2 = 1 \tag{7}$$

with *A*=9, *B*=8.7 and *C*=10. This is rendered in three dimensions below in Figure 9. The intensity of every point in this image is a linear function of the z value of the data; the lighter data points are closer to the z=0 plane. We define the range of the data to be x,y = [-3,3][-3,3].

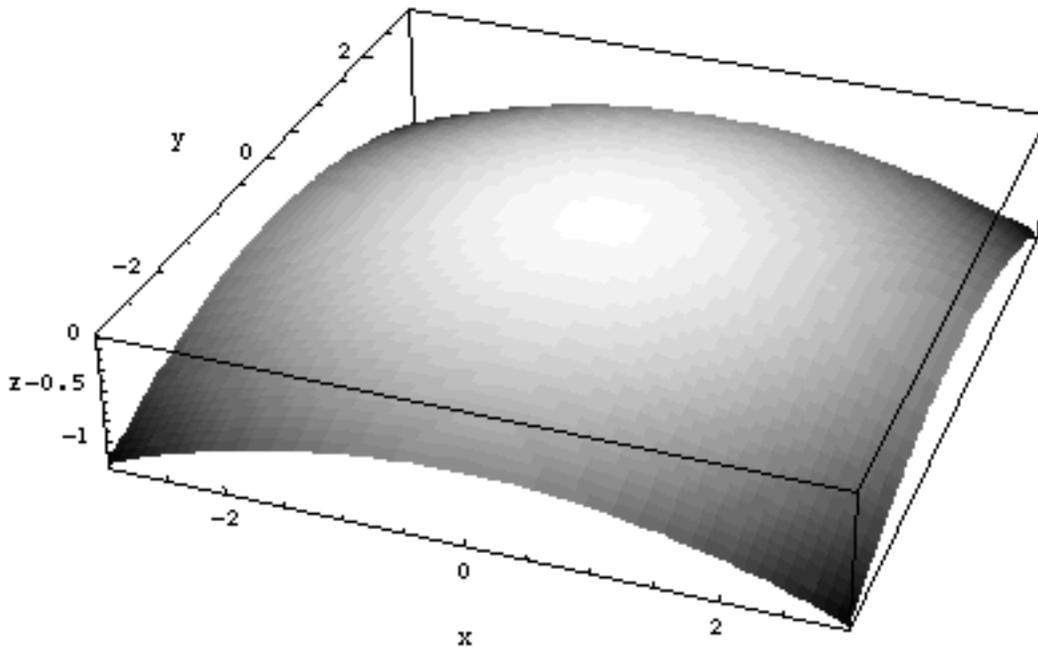Figure 9: A three-dimensional view of our simulated cornea, modeled as an ellipsoid with *A*=9, *B*=8.7 and *C*=10.

The most striking metric is axial refractive power. It highlights the inherent astigmatism associated with this asymmetric model. We can easily measure that there are four diopters of cylinder and the model is exactly with-the-rule. Retinal distance demonstrates that the left and right areas contribute to focus slightly better than the top and bottom regions, with a good focus in the central circle. Instantaneous refractive power and focusing distance indicate little here other than the focus is worse away from the center, and that the errors are close to rotationally symmetric.

4.2 Real Data

This data is from a patient with keratoconus[16,17,18], a condition in which the cornea has a local region of high curvature, which for this cornea is an oval region in the lower left of the image. This data was reconstructed from the ring patterns shown in Figure 1. Of our metrics, instantaneous refractive power and focusing distance highlight the keratoconus best. In fact, instantaneous refractive power gives similar values for the amount of curvature in the region as does instantaneous power, Gaussian power, and mean sphere. The axial refractive power map has a crescent shape because the keratoconus is eccentric and results in some astigmatism. Retinal distance, in conjunction with focusing distance, indicates which rays contribute to good focus. In this case, only a small central area provides a good focus, as this is the only area where both maps are near zero.
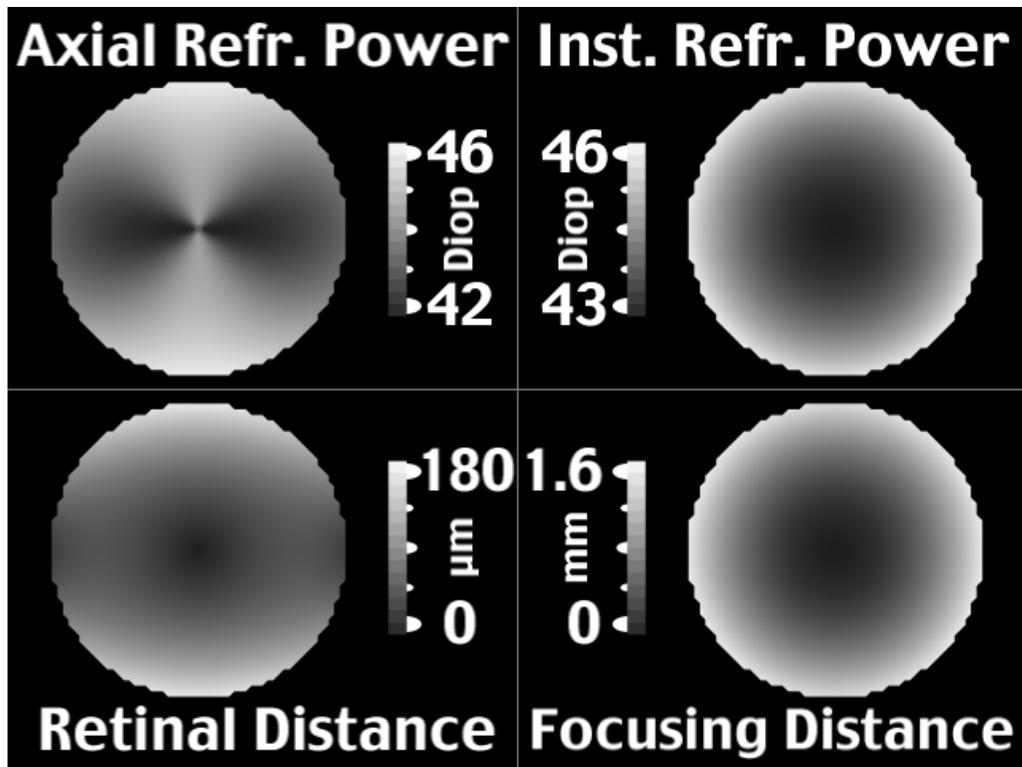
Figure 10: A view of our four acuity metrics for ellipsoidal simulated data.
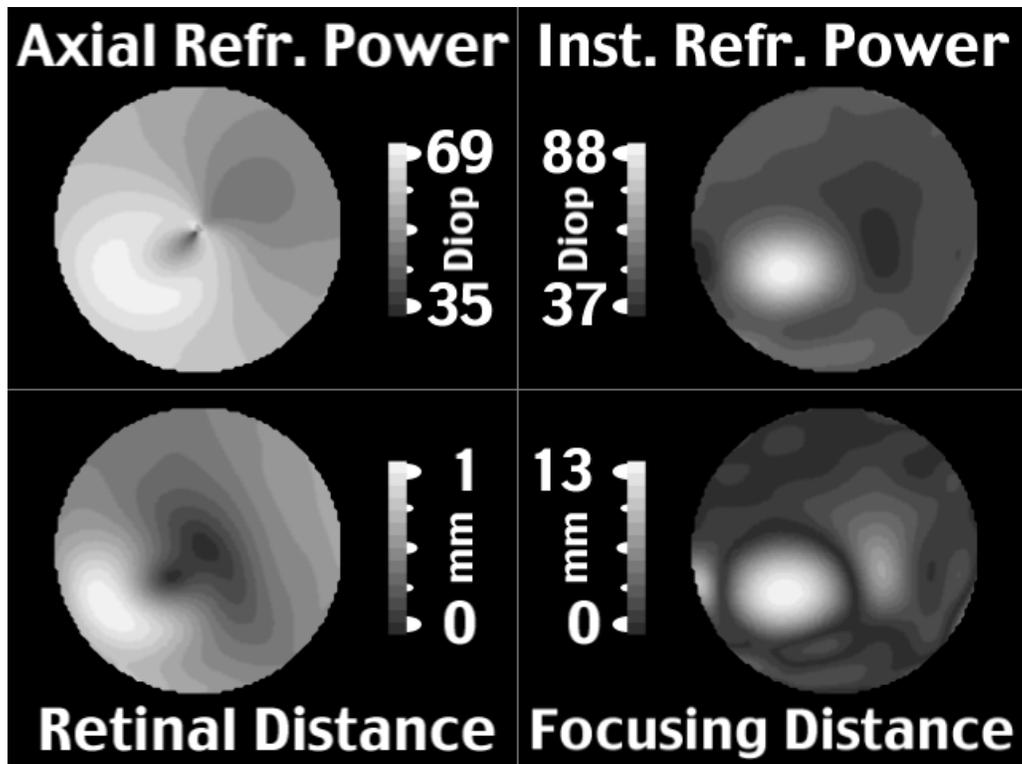

Figure 11: A view of our four acuity metrics for the real data of a keratoconic cornea.

5. CONCLUSION

We have presented four metrics for simulating visual acuity based on geometric optics, and showed the results using simulated and real data as implemented by CWhatUC. Axial refractive power is familiar to clinicians who often use a similar measure for astigmatism. Instantaneous refractive power is useful for describing the corneal shape, but doesn't take the PFP into account. Focusing distance and retinal distance taken together illustrate which regions contribute to a crisp focus onto the PFP. In summary, the four metrics, when used to supplement one another, provide additional insight into the prediction of a patient's visual acuity.

6. ACKNOWLEDGMENTS

7. REFERENCES

1. S. D. Klyce, "Computer-Assisted Corneal Topography, High-Resolution Graphic Presentation and Analysis of Keratoscopy", *Invest. Ophthalmol. Vis. Sci.* **25**, pp. 1426-1435, 1984.

2. D. D. Koch, G. N. Foulks, and T. Moran, "The Corneal Eyesys System: Accuracy, Analysis and Reproducibility of First Generation Prototype", *Refract. Corneal Surg.* **5**, pp. 424-429, 1989.

3. R. J. Mammone, M. Gersten, D. J. Gormley, R. S. Koplin, and V. L. Lubkin, "3-D Corneal Modeling System", *IEEE Trans. Biomedical Eng.* **37**, pp. 66-73, 1990.

4. J. Wang, D. A. Rice, and S. D. Klyce, "A New Reconstruction Algorithm for Improvement of Corneal Topographical Analysis", *Refract. Corneal Surg.* **5**, pp. 379-387, 1989.

5. S. E. Wilson and S. D. Klyce, "Advances in the Analysis of Corneal Topography", *Surv. Ophthalmol.* **35**, pp. 269-277, 1991.

6. M. A. Halstead, B. A. Barsky, S. A. Klein, and R. B. Mandell, "Reconstructing Curved Surfaces From Specular Reflection Patterns Using Spline Surface Fitting of Normals", *Proceedings of ACM/SIGGRAPH '96, New Orleans, 4-9 August 1996*, pp. 335-342, 1996.

7. M. A. Halstead, B. A. Barsky, S. A. Klein, and R. B. Mandell, "A Spline Surface Algorithm for Reconstruction of Corneal Topography from a Videokeratograph Reflection Pattern", *Optom. Vis. Sci.* **Vol 72, No. 11**, pp. 821-827, 1995.

8. O. Stavroudis, "Simpler Derivation of the Formulas for Generalized Ray Tracing", *J. Opt. Soc. Amer.* **Vol. 66, No. 12**, pp. 1330-1333, 1976.

9. J. E. A. Landgrave and J. R. Moya-Cessa, "Generalized Coddington Equations in Ophthalmic Lens Design", *J. Opt. Soc. Amer.* **Vol. 12, No. 8**, pp. 1637-1644, 1996.

10. S. A. Klein, R. B. Mandell, and B. A. Barsky, "Representing Corneal Shape" in *Vision Science and its Applications*. Technical Digest Series. Washington, DC: Optical Society of America, **vol. 1**, pp. 37-40, 1995.

11. R. B. Mandell, S. A. Klein, C. H. Shie, B. A. Barsky and Z. Yang. "Axial and Instantaneous Radii in Videokeratography". *Invest. Ophthalmol. Vis. Sci.* **35(Suppl)**, p. 2079, 1994.

12. C. Roberts. "The Accuracy of Power Maps to Display Curvature Data in Corneal Topography Systems". *Invest. Ophthalmol. Vis. Sci.* **35**, pp. 3525-3532, 1994.

13. R. Kumpf, "Multivariate Corneal Visualization in the EyeView System". *M. S. Thesis*, University of California at Berkeley, May 1995.

14. B. A. Barsky, S. A. Klein, and D. D. Garcia, "Gaussian Power with Cylinder Vector Field Representation for Corneal Topography Maps", *Optom. Vis. Sci.* **Vol. 74, No. 11**, pp 917-925, 1997.

15. B. A. Barsky, S. A. Klein, and D. D. Garcia, "Gaussian Power, Mean Sphere, and Cylinder Representations for Corneal Maps with Applications to the Diagnosis of Keratoconus", *Invest. Ophthalmol. Vis. Sci.* **37.** p. 558, 1996**.**

16. B. A. Barsky, R. B. Mandell, and S. A. Klein, "Corneal Shape Illusion in Keratoconus", *Invest. Ophthalmol. Vis. Sci.* **36 Suppl.**, p. 5308, 1995.

17. J. H. Krachmer, R. S. Feder, and M. W. Belin, "Keratoconus and Related Noninflammatory Corneal Thinning Disorders", *Surv. Ophthalmol.* **28,4**, pp. 293-322, 1984.

18. L. J. Maguire and W. D. Bourne, "Corneal Topography of Early Keratoconus", *Am. J. Ophthalmol.* **108**, pp. 107-112, 1989.